Cooperative Cold Denaturation: The Case of the C-Terminal Domain of Ribosomal Protein L9

ARTICLE *in* BIOCHEMISTRY · MARCH 2013

Impact Factor: 3.02 · DOI: 10.1021/bi3016789 · Source: PubMed

BIOCHEMISTRY
including biophysical chemistry & molecular biology

Article

pubs.acs.org/biochemistry

Cooperative Cold Denaturation: The Case of the C-Terminal Domain of Ribosomal Protein L9

Bowu Luan,[†] Bing Shan,[†] Carlos Baiz,[‡] Andrei Tokmakoff,[‡] and Daniel P. Raleigh*[,†,§]

[†]Department of Chemistry, Stony Brook University, Stony Brook, New York 11794-3400, United States

[‡]Department of Chemistry, Massachusetts Institute of Technology, Cambridge, Massachusetts 02139, United States

[§]Graduate Program in Biochemistry and Structural Biology and Graduate Program in Biophysics, Stony Brook University, Stony Brook, New York 11794-3400, United States

Supporting Information

ABSTRACT: Cold denaturation is a general property of globular proteins, but it is difficult to directly characterize because the transition temperature of protein cold denaturation, T_c, is often below the freezing point of water. As a result, studies of protein cold denaturation are often facilitated by addition of denaturants, using destabilizing pHs or extremes of pressure, or reverse micelle encapsulation, and there are few studies of cold-induced unfolding under near native conditions. The thermal and denaturant-induced unfolding of single-domain proteins is usually cooperative, but the cooperativity of cold denaturation is controversial. The issue is of both fundamental and practical importance because cold unfolding may reveal information about otherwise inaccessible partially unfolded states and because many therapeutic proteins need to be stabilized against cold unfolding. It is thus desirable to obtain more information about the process under nonperturbing conditions. The ability to access cold denaturation in native buffer is also very useful for characterizing protein thermodynamics, especially when other methods are not applicable. In this work, we study a point mutant of the C-terminal domain of ribosomal protein L9 (CTL9), which has a T_c above 0 °C. The mutant was designed to allow the study of cold denaturation under near native conditions. The cold denaturation process of I98A CTL9 was characterized by nuclear magnetic resonance, circular dichroism, and Fourier transform infrared spectroscopy. The results are consistent with apparently cooperative, two-state cold unfolding. Small-angle X-ray scattering studies show that the unfolded state expands as the temperature is lowered.

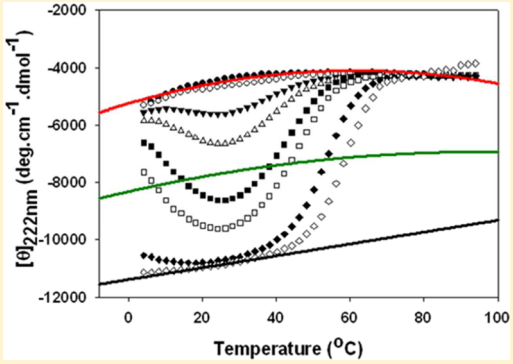

Protein cold denaturation, a transition from the folded state to an unfolded state induced by lowering the temperature from the temperature of maximal stability, is a general property of globular proteins. This phenomenon is predicted well by the Gibbs−Helmholtz equation and is rationalized by the decrease in the level of hydrophobic interactions together with solvation effects, including water penetration, although the details are still under debate.[1−5] There is evidence that cold denaturation is relevant *in vivo* and cold denaturation has important practical implications for the formulation of biotherapeutics.[6−11] For example, cold unfolding has been reported to affect monoclonal antibodies.[6−8] Proteins undergo ice−water surface denaturation, cold denaturation, and cryoconcentration, making it critical to carefully design freeze−thaw and storage conditions to maintain the activity of protein pharmaceuticals.[11] Studies of protein function in cold-adapted organisms have revealed a delicate balance between harsh environments (cold-induced denaturation) and catalytic activity (the compromise of structural flexibility).[9,10] Thus, a more detailed understanding of the process is of considerable practical importance.

Cold denaturation of amyloid has been reported,[12] indicating it is a general phenomenon. Interestingly, intrinsically disordered proteins (IDPs) have been suggested to be more resistant to cold treatment,[13] although this will likely depend on the particular protein under investigation. Cold denaturation has been proposed to provide access to important partially unfolded states that are otherwise inaccessible.[14−16] Analysis of the cold unfolding transition also allows one to characterize protein stability, especially for proteins whose thermal unfolding transitions are hard to measure.

Unfortunately, the transition temperature of cold denaturation is often well below the freezing point of an aqueous solution, making it difficult to study, and this has limited progress. Modifications to the system, such as adding denaturant, high pressure, extremes of pH, or encapsulating the protein of interest inside micelles, have allowed studies of the cold denatured state; however, those conditions are different from native buffer, and proteins may behave differently when subjected to strongly non-native conditions.

Received: December 19, 2012
Revised: March 3, 2013
Published: March 5, 2013

   dx.doi.org/10.1021/bi3016789 | *Biochemistry* 2013, 52, 2402−2409

Two-state, cooperative thermal and denaturant-induced unfolding is a common feature for small single-domain proteins; however, the cooperativity of cold denaturation is less well characterized and is controversial.[14−19] To gain more insight into the cooperativity of the protein cold denaturation process, it is desirable to study systems under near physiological conditions. A very limited number of such studies have been reported.[20−23] Here we characterize the cold unfolding of a globular protein in native buffer and show that it is an apparent two-state, cooperative process. A point mutant of the C-terminal domain of ribosomal protein L9 (CTL9) is used as a model protein in this work. The 92-residue domain adopts an $\alpha-\beta$ fold (Figure 1), and its thermal unfolding, pH-induced unfolding, and denaturant-induced unfolding have been well characterized and appear to be two-state processes.[24−26] The T_m is pH-dependent, in part because of several buried histidine side chains. The conformational properties of the cold unfolded state of the mutant have been examined at 12 °C;[27] however, the cooperativity of the transition has not been probed, nor have the properties of the cold unfolded state been analyzed in detail at lower temperatures.

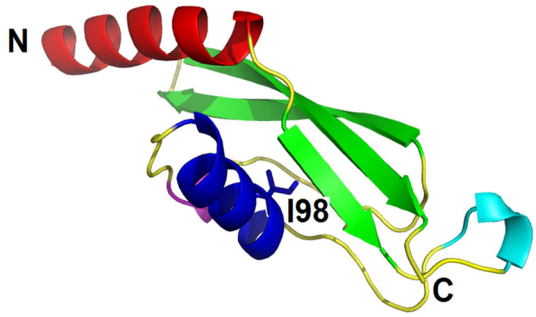

Figure 1. Ribbon diagram of CTL9. The β-sheet is colored green, the first α-helix red, and the second α-helix blue. The hydrophobic core residue I98 and the two termini are labeled. The Protein Data Bank entry is 1DIV. The diagram was constructed using PyMol.

EXPERIMENTAL PROCEDURES

Mutagenesis, Protein Expression, and Purification. I98A CTL9 was expressed and purified using procedures previously described for wild-type CTL9.[24,28] The identity of the protein was confirmed by DNA sequencing and MALDI-TOF mass spectrometry. The observed molecular mass was 9940.9 ± 1.2 Da, and the expected molecular mass was 9939.5 Da. The yield of the protein was 70−80 mg/L in LB medium and 30 mg/L in M9 minimal medium. A similar yield was observed for wild-type CTL9. The purity was tested by analytical HPLC.

Nuclear Magnetic Resonance (NMR) Experiments. ^{15}N-labeled I98A CTL9 was dissolved in 10% D_2O and 90% H_2O with 10 mM MOPS and 150 mM NaCl at a protein concentration of ∼1.0 mM. The pH was adjusted to 6.0. ^{15}N−^{1}H correlated heteronuclear single-coherence (HSQC) experiments were performed on a 600 MHz Varian spectrometer, from 5 to 25 °C with an increment of 3−4 °C. The temperature was calibrated using a standard methanol sample. ^{15}N−^{1}H HSQC spectra were recorded using 2048 × 512 complex points with 16 scans per increment and spectral widths of 8000.000 and 2199.978 Hz for the ^{15}N and ^{1}H dimensions, respectively. The ^{15}N offset frequency was set to 118.0 ppm, and the ^{1}H dimension was centered at the water resonance. The spectra were processed using NMRpipe[29] and visualized in NMRViewJ.[30] One-dimensional (1D) NMR experiments were performed on a sample containing 1.0 mM I98A CTL9 in 10 mM MOPS and 150 mM NaCl, dissolved in 100% D_2O with the pD adjusted to 5.6 (uncorrected pH meter reading). 2,2-Dimethyl-2-silapentane-5-sulfonate sodium salt (DSS, 0.5 mM) was used as an internal reference. The data were analyzed using the Mnova 7.

Circular Dichroism (CD) Spectroscopy. CD experiments were performed on a Chirascan CD spectrometer. The protein was dissolved in 10 mM MOPS and 150 mM NaCl buffer in D_2O, at a protein concentration of ∼20 μM. D_2O was used to allow comparison with the ^{1}H NMR spectra and FTIR experiment. Far-UV wavelength spectra were recorded in a 1 mm cuvette from 196 to 260 nm with a 1 nm increment and averaged with three repetitions. Thermal denaturation experiments were conducted as a function of pD between 4.0 and 8.0. Each thermal denaturation was performed by monitoring the ellipticity at 222 nm in a 1 cm cuvette, from 4 to 98 °C, with a 2 °C step and a heating rate of 1 °C/min. Singular-value decomposition (SVD) analysis was conducted using the program implemented in R version 2.13.0 (R, A language and environment for statistical computing. R Foundation for Statistical Computing, Vienna, Austria). The pD 4.0 thermal denaturation data were fit to a quadratic equation to obtain the unfolded state signal. The pD 8.0 curve was fit to the following equation to obtain thermodynamic parameters of the native state. The observed CD signal, $\theta(T)$, was fit to the equation

$$\theta(T) = \{a_n + b_nT + (a_d + b_dT)\exp[-\Delta G_u^\circ(T)/(RT)]\} / \{1 + \exp[-\Delta G_u^\circ(T)/(RT)]\} \quad (1)$$

where $\Delta G_u^\circ(T)$ is the free energy change upon thermal unfolding described by the Gibbs−Helmholtz equation:

$$\Delta G_u^\circ(T) = \Delta H^\circ(T_m) - T\Delta S^\circ(T_m) + \Delta C_p^\circ[T - T_m - T\ln(T/T_m)] \quad (2)$$

where a_n, b_n, a_d, and b_d are parameters that define the signals of the native state (N) and denatured state (D) as a function of temperature. T_m is the thermally induced unfolding midpoint temperature, and $\Delta H^\circ(T_m)$ is the enthalpy change at T_m. The signal expected for a fraction folded of 0.5 was estimated by taking the average of the native state baseline and the unfolded state baseline as a function of temperature.

Fourier transform infrared (FTIR) Experiments. Amide I IR spectra were recorded over the temperature range from 3 to 25 °C at 1 °C intervals, using a Nicolet 380 FTIR instrument with a resolution of 2 cm^{-1}. The sample cell consists of CaF_2 windows separated by a 50 μm PTFE spacer; 10 mM MOPS buffer with 150 mM NaCl in 100% D_2O (pD 5.6) was used for the FTIR measurements. The concentration of I98A CTL9 was 5.0 mg/mL. To account for the thermal shift of the amide I band, which is independent of structural changes in the protein, FTIR spectra were shifted by a phenomenological value of 0.052 cm^{-1}/°C with a reference temperature of 15 °C. Difference spectra were obtained by subtracting the final spectrum collected at 25 °C to obtain the difference between the native and DSE FTIR contributions. SVD was performed on the equilibrium spectra to project out the spectral response, and the temperature profile associated with the cold denaturation of CTL9.

dx.doi.org/10.1021/bi3016789 | Biochemistry 2013, 52, 2402−2409

Small-Angle X-ray Scattering (SAXS) Measurements. Samples of I98A CTL9 were prepared in buffer consisting of 10 mM MOPS and 150 mM NaCl in 100% H_2O, with the pH adjusted to 6.0. Scattering experiments were performed at beamline X9 at Brookhaven National Laboratory, National Synchrotron Light Source I (Upton, NY). Protein samples were injected into a 1 mm capillary continuously during the measurement at a rate of 0.67 μL/s to avoid radiation damage. The exposure time for each measurement was 30 s. Scattering data were collected for I98A CTL9 at a protein concentration of 3.75 mg/mL, at 7, 12, and 25 °C. Each sample was measured three times and then averaged before data analysis. The program pyXS (http://www.bnl.gov/ps/x9/software/pyXS.asp) was used for buffer subtraction, and the radius of gyration (R_g) was obtained using the Guinier approximation using PRIMUS[31]

$$I(q) = I(0) \times \exp(-R_g^2 q^{2/3}) \quad (3)$$

where $I(q)$ is the intensity at scattering vector q.[32]

RESULTS

I98A CTL9 Undergoes Cold Denaturation under Near Native Conditions, with a T_c above 0 °C. We used a designed core mutant of CTL9, chosen to destabilize the protein without perturbing its fold, or the two-state nature of the high-temperature unfolding transition.[27] I98 lies in the hydrophobic core of the protein (Figure 1), and its truncation to a smaller hydrophobic residue destabilizes the domain by reducing the hydrophobic driving force for folding and by altering core packing. The I98A mutant destabilizes CTL9 by ~4 kcal/mol. The temperature of cold denaturation increases as ΔC_p° increases and as $\Delta H^\circ(T_m)$, the enthalpy change at the midpoint of thermal unfolding, decreases. The I98A mutant was chosen because the altered core packing was expected to decrease $\Delta H^\circ(T_m)$.[26]

The mutation was also designed to increase ΔC_p° by potentially weakening hydrophobic clusters in the unfolded state.[26] The structure of the mutant is the same as that of the wild type, as suggested by CD and NMR chemical shift analysis. The classical approach for probing the cooperativity of folding or unfolding is to use two or more distinct, structurally sensitive, spectroscopic methods. Different structural probes will yield overlapping transition curves if only two distinct structural states are well populated during the protein folding process.[33,34] In this work, we use NMR, CD, and FTIR to follow the unfolding of the I98A mutant.

$^{15}N-^{1}H$ HSQC spectra were collected for the I98A CTL9 mutant at 5 and 25 °C at pH 6.0 (Figure 2). The resonances due to the unfolded state have limited dispersion in both the ^{15}N and ^{1}H dimensions, which is typical of an unfolded protein ensemble. At low temperatures, the peaks from the denatured state ensemble (DSE) are much more intense than those from the folded state, indicating that the DSE is the dominant species under these conditions. Peaks from the folded state can be observed even in the 5 °C spectrum at lower contour levels. The line widths are sharp, suggesting that the protein is monomeric, in agreement with hydrodynamic measurements.[26] The peaks of the DSE at 25 °C match well with those of the cold denatured state at low temperatures. Most of the native resonances in the 25 °C HSQC spectrum of the mutant are not shifted relative to their position in the spectrum of the folded wild-type protein,[27] indicating that the mutation does not significantly perturb the structure. No obvious broadening of the resonances is detected for any of the peaks, demonstrating that the two states are in slow exchange on the NMR chemical shift time scale.

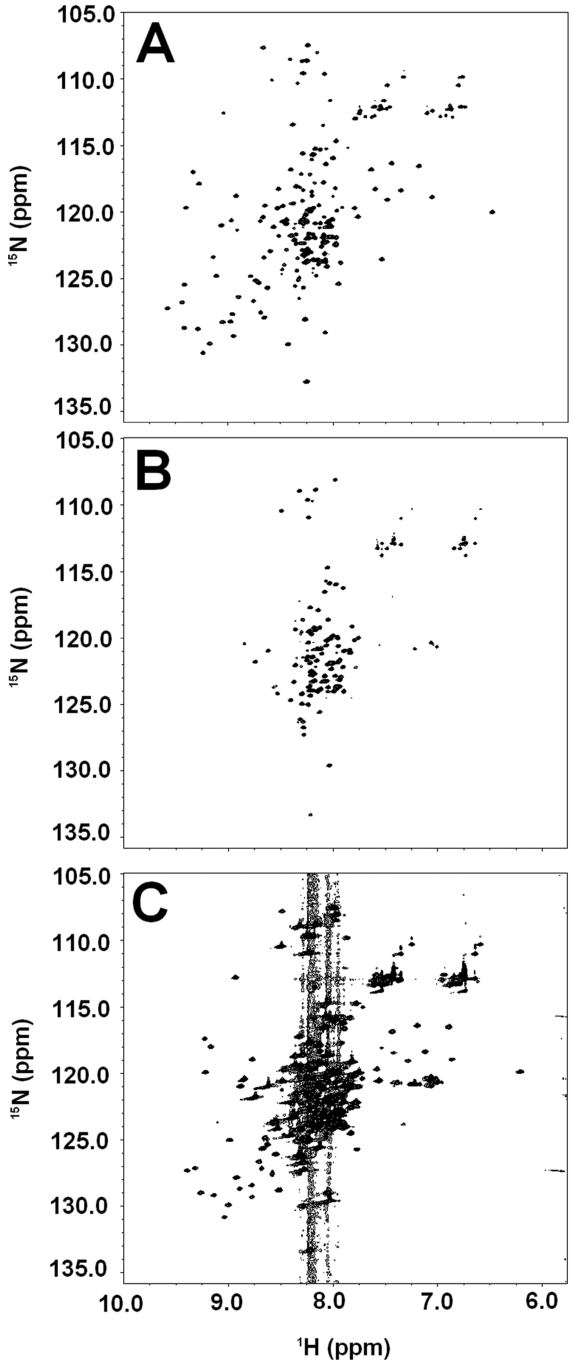

Figure 2. $^{15}N-^{1}H$ HSQC spectra of I98A CTL9 at pH 6.0, in 10 mM MOPS and 150 mM NaCl buffer, 10% D_2O, and 90% H_2O at (A) 25 and (B) 5 °C. (C) The 5 °C spectra plotted at a lower contour level to visualize the folded state resonances.

Like that of wild-type CTL9, the stability of the I98A mutant depends strongly on pH. The protein becomes less stable when the histidine side chains are protonated at lower pH and is more stable when the histidine side chains are deprotonated. Figure 3 shows thermal unfolding curves for I98A CTL9 at different pD values detected by CD. D_2O is used for these studies to allow direct comparisons with FTIR and ^{1}H NMR.

dx.doi.org/10.1021/bi3016789 | Biochemistry 2013, 52, 2402−2409

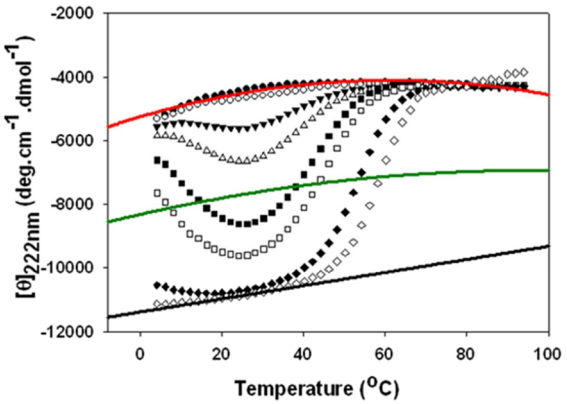

Figure 3. CD-detected thermal unfolding curves for I98A CTL9 monitored at different pD values for protein dissolved in 10 mM MOPS and 150 mM NACl in D_2O at (●) pD 4.0, (○) 4.7, (▼) 5.2, (△) 5.4, (■) 5.6, (□) 6.0, (◆) 6.6, and (◇) 8.0. Note the strong dependence of the transitions on pD. The red curve represents a quadratic fit to the pD 4.0 data and provides an experimental estimation of the unfolded state signal as a function of temperature because the fraction folded equals 0 under these conditions. The pD 8.0 data provide an estimation of the CD signal for the fully folded state as the fraction folded equals 1.0 at 25 °C and pD 8.0. The solid black line represents an extrapolation of the folded baseline. The green curve represents the signal expected for a fraction folded of 0.5, i.e., the midpoint of the transition.

Cold denaturation is observed between pD 4.7 and 6.6. The shape of the curves is similar to the shape of those observed in H_2O,[27] although the transition temperatures are shifted. The red curve represents a quadratic fit to the pD 4.0 data and provides an experimental estimation of the DSE signal as a function of temperature, because the fraction folded is zero under these conditions. The pD 8.0 data provide an estimation of the CD signal for the fully folded state as the fraction folded equals 1 at 25 °C and pD 8.0. The solid black line represents an extrapolation of the folded baseline. The green curve represents the signal expected for a fraction folded of 0.5, i.e., the midpoint of the transition. On the basis of this data set, the fraction folded (or unfolded) can be easily calculated at a given temperature and pD. At pD 5.6, the population of the cold denatured ensemble is 76% at 4 °C, and at 25 °C, the native state and the DSE are populated to 64 and 36%, respectively.

CD, FTIR, and NMR Are Consistent with Two-State, Cooperative Cold Denaturation. Far-UV CD spectra of I98A CTL9 were recorded over the temperature range of 2−25 °C (Figure 4). Data were collected in D_2O to allow comparison with FTIR and 1D ^{1}H NMR measurements. D_2O can stabilize proteins, so it is important to match the isotopic composition of the solvent.[35,36] The spectrum at 25 °C indicates a mixture of α-helix, β-strand, and coil. Below 10 °C, the spectra are typical of those expected for an unfolded protein but do not correspond to a classic random coil. In particular, there is still significant intensity at 222 nm, consistent with the presence of residual helical structure. An isodichroic point at 207 nm is observed during cold unfolding, consistent with a two-state transition. An isodichroic point is a necessary but not a sufficient condition for a two-state transition. Single-value decomposition (SVD) analysis shows that only two major spectral components are needed to define the transition: the second component is weighted 12% relative to the largest component, the third contributes 1.1%, and all of the other components are negligible.

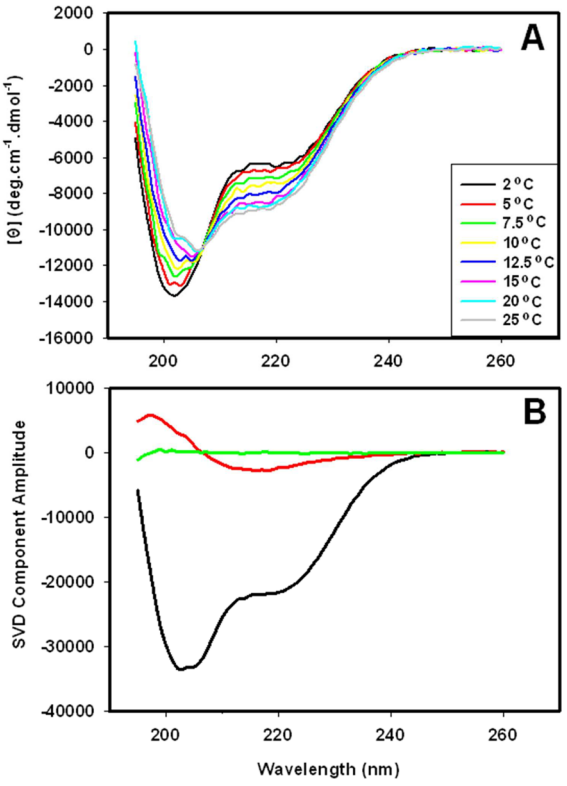

Figure 4. (A) Far-UV CD spectra of the I98A CTL9 mutant as a function of temperature, recorded over the temperature range from 2 to 25 °C at pD 5.6, in 10 mM MOPS and 150 mM NaCl. (B) Results of the SVD analysis for the temperature-dependent unfolding of I98A CTL9 monitored by CD. The relative amplitudes of the first (black), second (red), and third (green) components are 1.00, 0.120, and 0.011, respectively.

FTIR data were collected for the I98A CTL9 mutant over the temperature range of 3−25 °C in D_2O (Figure 5). An isosbestic point is observed, and SVD analysis of the FTIR data shows that only two significant components are required to describe the difference spectra. The second and third component weights are 0.92 and 0.28% of that of the first component, respectively. Difference spectra show a loss feature at ∼1618 cm^{-1}, typically associated with proline turns and β-structure, as well as a gain in the 1630 cm^{-1} region, normally associated with the strong ν perpendicular mode of antiparallel β-sheets.[37,38] A pronounced loss of intensity around 1650 cm^{-1} can be attributed to modes arising from α-helices and disordered regions. The spectra indicate that the DSE contains β-sheet character, and decreased α-helix content in comparison to that of the native structure.

The aromatic region of the ^{1}H NMR spectra of I98A CTL9 displays well-resolved peaks from tyrosine resonances of the native state and the DSE (Supporting Information). The single tyrosine is at residue 126, which is located in the second α-helix. Integration of the area under the unfolded and folded tyrosine peaks provides an independent estimate of the fraction unfolded as a function of temperature. The values are in good agreement with the ones obtained by CD, consistent with a two-state process (Figure 6).

As a control, we compared pD-induced unfolding at 25 °C to thermal unfolding experiments at different pD values. This produces a test of the reliability of the parameters extrapolated from the thermal unfolding data. Each thermal unfolding curve

dx.doi.org/10.1021/bi3016789 | Biochemistry 2013, 52, 2402−2409

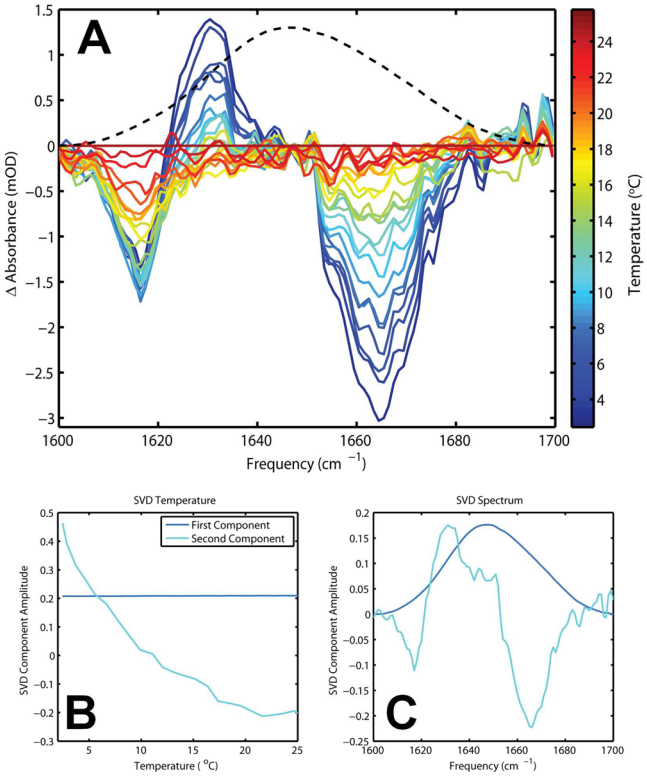

Figure 5. (A) Difference FTIR spectra of I98A CTL9 at pD 5.6 from 3 to 25 °C. The 25 °C data were subtracted from the data collected at different temperatures. (B) The temperature dependence of the SVD components suggests that the first component is constant, and the second component shows a monotonic decrease, which is consistent with cooperative cold unfolding. (C) SVD analysis of the FTIR data shows two major components for the cold denaturation of I98A CTL9. The relative amplitudes of the first (blue) and second (cyan) components are 1.00 and 0.00921, respectively. The relative amplitude of the third component (not shown) is 0.00282.

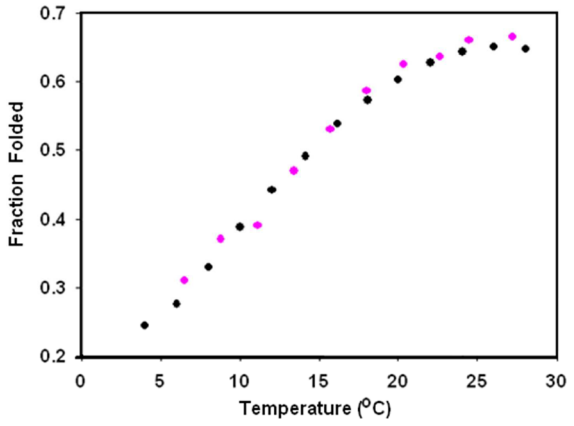

Figure 6. Estimation of the fraction folded vs temperature based on CD data (black circles) calculated from the CD temperature melting curve at pD 5.6 and NMR data (magenta circles) calculated from the relative peak intensities of the Y126 resonance from unfolded and folded states. Experiments were performed as a function of temperature in 10 mM MOPS and 150 mM NaCl (pD 5.6) in 100% D_2O.

was analyzed using the Gibbs–Helmholtz equation to obtain the thermodynamic parameters at 25 °C. There is excellent agreement between these values and the values obtained by the pD titration unfolding curve (Figure 7). The strong agreement indicates that the population estimates obtained from

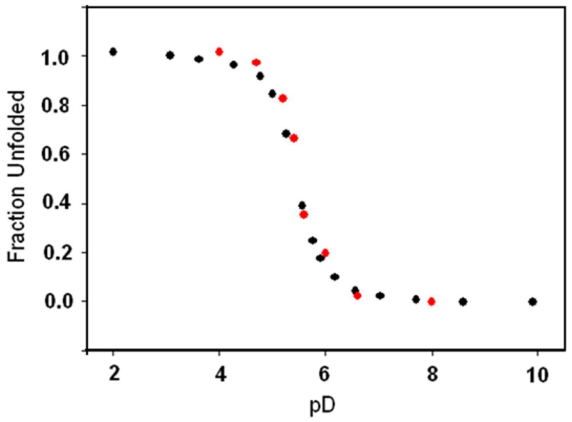

Figure 7. pD-induced denaturation of I98A CTL9. The CD signal at 222 nm was monitored in 10 mM MOPS and 150 mM NaCl in D_2O. The pD values were adjusted by adding DCl and NaOD directly to the cuvette: (black circles) calculated from the pD titration curve and (red circles) calculated from the extrapolation of thermal unfolding curves collected as a function of pD. The good agreement validates the extrapolation of the thermal unfolding data and suggests that the population estimates are precise, and that the unfolding is two-state.

extrapolation of the thermal unfolding curves are precise. The agreement is also consistent with two-state unfolding.

Small-Angle X-ray Scattering Data Show That the Cold Denatured State Expands at Low Temperatures. To further characterize the cold denatured state of I98A CTL9, we collected SAXS data at 7, 12, and 25 °C. The populations of the native state at those temperatures are 36, 50, and 65%, respectively. We used two methods to estimate the R_g of the DSE of I98A CTL9. First, we used the experimental curve and subtracted the scattering profile for the native state. Subtraction of the signal of the native state allows R_g of unfolded I98A CTL9 to be estimated. The folded state curve was collected independently for the fully folded state of wild-type CTL9 (Figure 8) and was subtracted, with appropriate weighting,

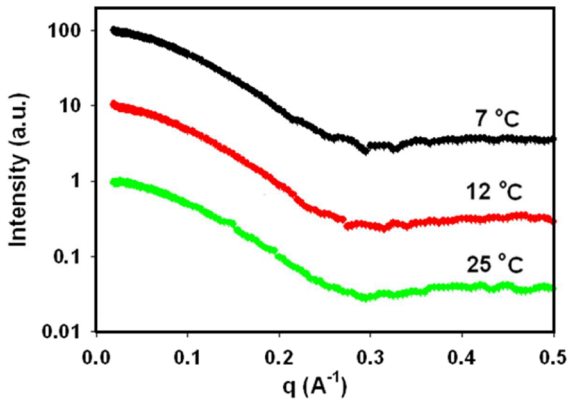

Figure 8. Scattering curves from wild-type CTL9 (control experiments) at 7 (black circles), 12 (red circles), and 25 °C (green circles). No apparent change in the shape of the curve was observed as a function of temperature, and the calculated R_g values are in excellent agreement, ranging from 14.9 ± 0.3 to 15.2 ± 0.3 Å. The curves are offset from each other for the sake of clarity. The buffer consisted of 10 mM MOPS and 150 mM NaCl, in H_2O.

dx.doi.org/10.1021/bi3016789 | *Biochemistry* 2013, 52, 2402–2409

from the experimental curve of I98A CTL9. The second method estimated the R_g for the DSE using the standard relationship for a two-component system:

$$R_g^2{}_{observed} = p_{native} R_g^2{}_{native} + p_{DSE} R_g^2{}_{DSE} \quad (4)$$

where p_{native} is the population of the native state and p_{DSE} is the population of the DSE ensemble.[39] Using the known R_g value for the native state provided by wild-type CTL9 and the relative populations of the native and DSE allows the R_g of the DSE to be estimated. The two approaches give estimates that are in very good agreement (Table 1). The cold denatured state expands, as judged by R_g, as the temperature is lowered, increasing by 17−27% as the temperature is reduced from 25 to 7 °C. The increase is significant and larger than the estimated uncertainty. This confirms previous hydrodynamic studies of I98A CTL9.[26] Control experiments show that the value of R_g for the folded state is independent of temperature (Figure 8).

Table 1. R_g Values for I98A CTL9

temp (°C)	R_g, folded (Å)[a]	R_g, unfolded (Å)[b]	R_g, unfolded (Å)[c]
7	15.2 ± 0.3	28.4 ± 0.9	28.2 ± 1.4
12	14.8 ± 0.4	26.1 ± 1.1	25.1 ± 1.6
25	14.5 ± 0.3	24.0 ± 1.1	22.2 ± 1.7

[a]Measured using wild-type CTL9. [b]Calculated from the observed scattering curve after subtraction of the folded state scattering curve. [c]Calculated from the equation $R_g^2{}_{observed} = p_{native} R_g^2{}_{native} + p_{DSE} R_g^2{}_{DSE}$, where p_{native} and p_{DSE} are the fractional populations of the native state and the DSE, respectively.

DISCUSSION

The denaturant-induced and thermally induced unfolding of globular single-domain proteins is usually cooperative, but the cooperativity of cold denaturation is less certain. The Yfh1 protein, a small $\alpha-\beta$ protein, undergoes two-state cold unfolding; however, deviations from two-state cold unfolding have been reported for ubiquitin encapsulated in reverse micelles.[14−16,20−22] Temperature-dependent NMR, CD, and FTIR experiments, together with SVD analysis, are all consistent with cooperative cold denaturation of I98A CTL9 in native buffer.

Why do the results reported here differ from the results of studies of ubiquitin encapsulated in reverse micelles? There may be fundamental differences in the behavior of the two proteins, although the equilibrium thermal unfolding of both has been reported to be cooperative in homogeneous solution. It has been suggested that studies in reverse micelles can be complicated by temperature-dependent interactions between the protein and the micelle or by water shedding.[18,40] PFG-NMR diffusion experiments[26] and the SAXS data reported here demonstrate that the cold denatured states of proteins can expand at low temperatures, which may enhance the opportunity for interactions between the micelle and the protein. Halle and co-workers have monitored the hydration dynamics of ubiquitin in nonperturbing picoliter emulsion droplets using ^{17}O-labeled water spin relaxation.[5] Ubiquitin was found to be thermodynamically stable even at −32 °C, suggesting that the cold denaturation of ubiquitin encapsulated in reverse micelles might be induced by the low water content of the micelles rather than by low temperatures. Irrespective of the details of previous studies, this work produces a system in which cold unfolding can be observed in native buffer.

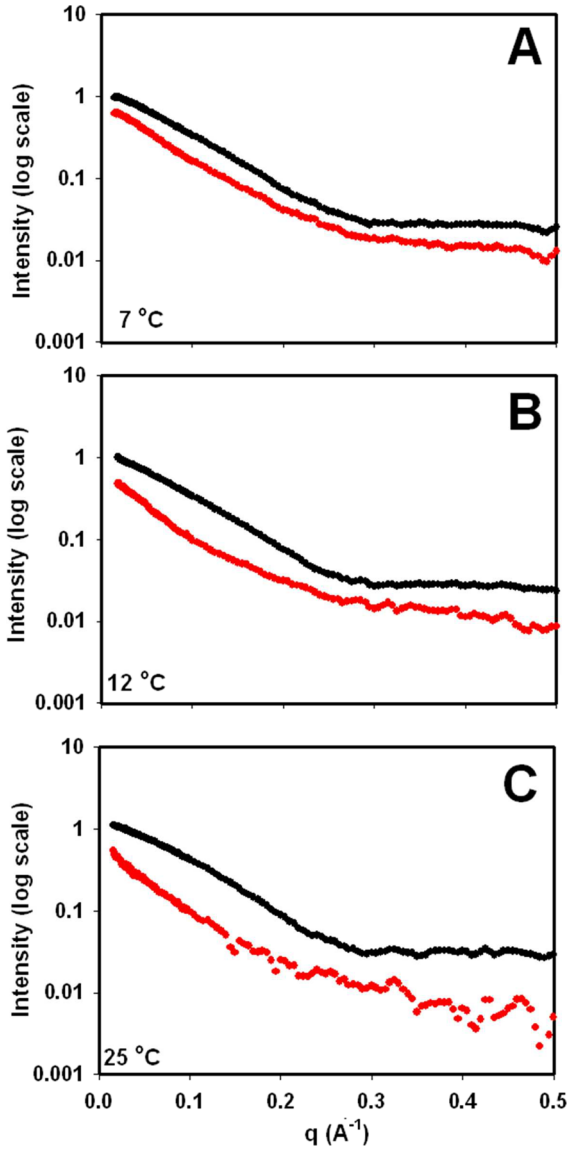

Figure 9. Observed scattering curves for I98A CTL9 (black circles) and the profile after subtraction (red circles) of the contribution of the folded ensemble at (A) 7, (B) 12, and (C) 25 °C.

The cooperativity of cold unfolding is important from a basic protein thermodynamics perspective, but it also has practical implications. Protein cold denaturation is an issue in the food processing industry, in cryopreservation, and in protein pharmaceuticals. Protein-based therapeutics are usually stored at low temperatures, and there have been reports of the cold denaturation of monoclonal antibodies.[6−8] Thus, designing resistance to cold-induced unfolding is of practical interest. It is conceptually easier to stabilize a cooperatively folded system rather than ones that fold noncooperatively. In the former, the effects of a mutation contribute to global stability, while in the latter, substitutions may impact the local stability of small portions of the structure but not affect other regions. It is clearly more challenging to design mutations that stabilize the native ensemble for the latter class of protein.

The CTL9 mutant analyzed here and Yfh1, at low salt concentrations, appear to undergo cooperative cold unfolding in native buffer in the absence of denaturation.[23] Whether

dx.doi.org/10.1021/bi3016789 | Biochemistry 2013, 52, 2402−2409

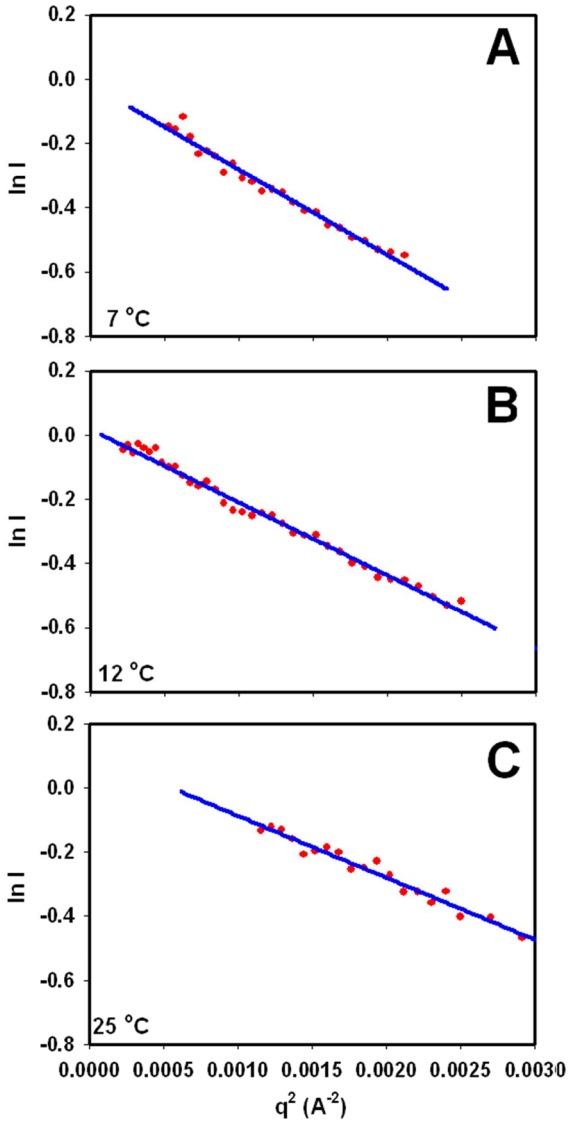

Figure 10. Guinier analysis of the profiles shown in Figure 9. Scattering profiles for the cold denatured ensembles (red circles) are shown. The Guinier approximation is shown as a blue straight line: (A) 7, (B) 12, and (C) 25 °C.

cooperative cold denaturation is a general property of globular proteins remains to be determined.

■ ASSOCIATED CONTENT

Supporting Information

Figure S1. This material is available free of charge via the Internet at http://pubs.acs.org.

■ AUTHOR INFORMATION

Corresponding Author

*E-mail: daniel.raleigh@stonybrook.edu. Phone: (631) 632-9547. Fax: (631) 632-7960.

Funding

Supported by National Science Foundation Grants MCB-0919860 to D.P.R. and CHE-1212557 to A.T.

Notes

The authors declare no competing financial interest.

■ ACKNOWLEDGMENTS

We thank Dr. Vadim Patsalo for helpful discussions and performing the SVD analysis of the far-UV CD data and Dr. Marc Allaire for the help of SAXS experiments. Use of the National Synchrotron Light Source, Brookhaven National Laboratory, was supported by the U.S. Department of Energy, Office of Science, Office of Basic Energy Sciences, under Contract DE-AC02-98CH10886.

■ ABBREVIATIONS

CD, circular dichroism; CTL9, C-terminal domain of the ribosomal protein L9 from *Bacillus stearothermophilus*; DSE, denatured state ensemble; DSS, 2,2-dimethyl-2-silapentane-5-sulfonate sodium salt; FTIR, Fourier transform infrared spectroscopy; HPLC, high-performace liquid chromatography; HSQC, heteronuclear single-quantum coherence; MALDI-TOF, matrix-assisted laser desorption ionization time-of-flight; MOPS, 3-(*N*-morpholino)propanesulfonic acid; PFG-NMR, pulsed field gradient nuclear magnetic resonance; R_g, radius of gyration; R_h, radius of hydration; SAXS, small-angle X-ray scattering; SVD, singular-value decomposition; T_c, temperature at the midpoint of cold unfolding; T_m, temperature at the midpoint of thermal unfolding.

■ REFERENCES

(1) Graziano, G. (2010) On the molecular origin of cold denaturation of globular proteins. *Phys. Chem. Chem. Phys. 12*, 14245−14252.

(2) Yoshidome, T., and Kinoshita, M. (2009) Hydrophobicity at low temperatures and cold denaturation of a protein. *Phys. Rev. E 79*, 030905 (R).

(3) Dias, C. L. (2012) Unifying microscopic mechanism for pressure and cold denaturations of proteins. *Phys. Rev. Lett. 109*, 048104.

(4) Dias, C. L., Ala-Nissila, T., Karttunen, M., Vattulainen, I., and Grant, M. (2008) Microscopic mechanism for cold denaturation. *Phys. Rev. Lett. 100*, 118101.

(5) Davidovic, M., Mattea, C., Qvist, J., and Halle, B. (2009) Protein cold denaturation as seen from the solvent. *J. Am. Chem. Soc. 131*, 1025−1036.

(6) Todgham, A. E., Hoaglund, E. A., and Hofmann, G. E. (2007) Is cold the new hot? Elevated ubiquitin-conjugated protein levels in tissues of Antarctic fish as evidence for cold-denaturation of proteins *in vivo*. *J. Comp. Physiol., B 177*, 857−866.

(7) Lazar, K. L., Patapoff, T. W., and Sharma, V. K. (2010) Cold denaturation of monoclonal antibodies. *mAbs 2*, 42−52.

(8) Feller, G. (2010) Protein stability and enzyme activity at extreme biological temperatures. *J. Phys.: Condens. Matter 22*, 323101.

(9) Pucciarelli, S., Parker, S. K., Detrich, H. W., III, and Melki, R. (2006) Characterization of the cytoplasmic chaperonin containing TCP-1 from the Antarctic fish *Notothenia coriiceps*. *Extremophiles 10*, 537−549.

(10) Hayley, M., Chevaldina, T., and Heeley, D. H. (2011) Cold adaptation of tropomyosin. *Biochemistry 50*, 6559−6566.

(11) Kolhe, P., and Badkar, A. (2011) Protein and solute distribution in drug substance containers during frozen storage and post-thawing: A tool to understand and define freezing-thawing parameters in biotechnology process development. *Biotechnol. Prog. 27*, 494−504.

(12) Kim, H. Y., Cho, M. K., Riedel, D., Fernandez, C. O., and Zweckstetter, M. (2008) Dissociation of amyloid fibrils of α-synuclein in supercooled water. *Angew. Chem., Int. Ed. 47*, 5046−5048.

(13) Tantos, A., Friedrich, P., and Tompa, P. (2009) Cold stability of intrinsically disordered proteins. *FEBS Lett. 583*, 465−469.

(14) Babu, C. R., Hilser, V. J., and Wand, A. J. (2004) Direct access to the cooperative substructure of proteins and the protein ensemble via cold denaturation. *Nat. Struct. Mol. Biol. 11*, 352−357.

(15) Whitten, S. T., Kurtz, A. J., Pometun, M. S., Wand, A. J., and Hilser, V. J. (2006) Revealing the nature of the native state ensemble through cold denaturation. *Biochemistry 45*, 10163−10174.
(16) Pometun, M. S., Peterson, R. W., Babu, C. R., and Wand, A. J. (2006) Cold denaturation of encapsulated ubiquitin. *J. Am. Chem. Soc. 128*, 10652−10653.
(17) Tian, J. H., and Garcia, A. E. (2011) Simulations of the confinement of ubiquitin in self-assembled reverse micelles. *J. Chem. Phys. 134*, 225101.
(18) Van Horn, W. D., Simorellis, A. K., and Flynn, P. F. (2005) Low-temperature studies of encapsulated proteins. *J. Am. Chem. Soc. 127*, 13553−13560.
(19) Kitahara, R., Okuno, A., Kato, M., Taniguchi, Y., Yokoyama, S., and Akasaka, K. (2006) Cold denaturation of ubiquitin at high pressure. *Magn. Reson. Chem. 44*, S108−S113.
(20) Adrover, M., Esposito, V., Martorell, G., Pastore, A., and Temussi, P. A. (2010) Understanding cold denaturation: The case study of Yfh1. *J. Am. Chem. Soc. 132*, 16240−16246.
(21) Adrover, M., Martorell, G., Martin, S. R., Urosev, D., Konarev, P. V., Svergun, D. I., Daura, X., Temussi, P., and Pastore, A. (2012) The role of hydration in protein stability: Comparison of the cold and heat unfolded states of yfh1. *J. Mol. Biol. 417*, 413−424.
(22) Martin, S. R., Esposito, V., Rios, P. D. L., Pastore, A., and Temussi, P. A. (2008) Cold denaturation of yeast frataxin offers the clue to understand the effect of alcohols on protein stability. *J. Am. Chem. Soc. 130*, 9963−9970.
(23) Pastore, A., Martin, S. R., Politou, A., Kondapalli, K. C., Stemmler, T., and Temussi, P. A. (2007) Unbiased cold denaturation: Low- and high-temperature unfolding of yeast frataxin under physiological conditions. *J. Am. Chem. Soc. 129*, 5374−5375.
(24) Sato, S., and Raleigh, D. P. (2002) pH-dependent stability and folding kinetics of a protein with an unusual α-β topology: The C-terminal domain of the ribosomal protein L9. *J. Mol. Biol. 318*, 571−582.
(25) Sato, S., Kuhlman, B., Wu, W. J., and Raleigh, D. P. (1999) Folding of the multidomain ribosomal protein L9: The two domains fold independently with remarkably different rates. *Biochemistry 38*, 5643−5650.
(26) Li, Y., Shan, B., and Raleigh, D. P. (2007) The cold denatured state is compact but expands at low temperatures: Hydrodynamic properties of the cold denatured state of the C-terminal domain of L9. *J. Mol. Biol. 368*, 256−262.
(27) Shan, B., McClendon, S., Rospigliosi, C., Eliezer, D., and Raleigh, D. P. (2010) The cold denatured state of the C-terminal domain of protein L9 is compact and contains both native and non-native structure. *J. Am. Chem. Soc. 132*, 4669−4677.
(28) Li, Y., Gupta, R., Cho, J. H., and Raleigh, D. P. (2007) Mutational analysis of the folding transition state of the C-terminal domain of ribosomal protein L9: A protein with an unusual β-sheet topology. *Biochemistry 46*, 1013−1021.
(29) Delaglio, F., Grzesiek, S., Vuister, G. W., Zhu, G., Pfeifer, J., and Bax, A. (1995) NMRpipe: A multidimensional spectral processing system based on Unix pipes. *J. Biomol. NMR 6*, 277−293.
(30) Johnson, B. A. (2004) Using NMRView to visualize and analyze the NMR spectra of macromolecules. *Methods Mol. Biol. 278*, 313−352.
(31) Konarev, P. V., Volkov, V. V., Sokolova, A. V., Koch, M. H. J., and Svergun, D. I. (2003) PRIMUS: A Windows PC-based system for small-angle scattering data analysis. *J. Appl. Crystallogr. 36*, 1277−1282.
(32) Guinier, A., and Fournet, G. (1955) *Small Angle Scattering of X-rays*, Wiley, New York.
(33) Chan, H. S., Shimizu, S., and Kaya, H. (2004) Cooperativity principles in protein folding. *Methods Enzymol. 380*, 350−379.
(34) Barrick, D. (2009) What have we learned from the studies of two-state folders, and what are the unanswered questions about two-state protein folding? *Phys. Biol. 6*, 015001.
(35) Makhatadze, G. I., Clore, G. M., and Gronenborn, A. M. (1995) Solvent isotope effect and protein stability. *Nat. Struct. Biol. 2*, 852−855.
(36) Kresheck, G. C., Schneider, H., and Scheraga, H. A. (1965) The effect of D_2O on the thermal stability of proteins. Thermodynamic parameters for the transfer of model compounds from H_2O to D_2O. *J. Phys. Chem. 69*, 3132−3144.
(37) Baiz, C. R., Peng, C. S., Reppert, M. E., Jones, K. C., and Tokmakoff, A. (2012) Coherent two-dimensional infrared spectroscopy: Quantitative analysis of protein secondary structure in solution. *Analyst 137*, 1793−1799.
(38) Volkov, V., and Hamm, P. (2004) A two-dimensional infrared study of localization, structure, and dynamics of a dipeptide in membrane environment. *Biophys. J. 87*, 4213−4225.
(39) Choy, W. Y., Mulder, F. A., Crowhurst, K. A., Muhandiram, D. R., Millett, I. S., Doniach, S., Forman-Kay, J. D., and Kay, L. E. (2002) Distribution of molecular size within an unfolded state ensemble using small-angle X-ray scattering and pulse field gradient NMR techniques. *J. Mol. Biol. 316*, 101−112.
(40) Simorellis, A. K., Van Horn, W. D., and Flynn, P. F. (2006) Dynamics of low temperature induced water shedding from AOT reverse micelles. *J. Am. Chem. Soc. 128*, 5082−5090.